

Localization

Kegen Yu, Harri Saarnisaari, Jean-philippe Montillet, Alberto Rabbachin,

Ian Oppermann and Giuseppe Thadeu Freitas de Abreu

Centre for Wireless Communications

University of Oulu, Finland

1 Introduction

Precision localization has been one of the fascinating application areas for impulse radio ultra wideband (IR-UWB) technology. These applications exploit the fine time resolution of UWB signals. The ultra short pulse waveform enables UWB receivers accurately determine the time-of-arrival (TOA) of the signal transmitted from another UWB transmitter. For example, the accuracy of TOA measurements has been made better than 40 picoseconds [1], which corresponds to 1.2 centimeters spatial uncertainty.

There are various existing/potential applications of precision localization by making use of UWB technology. A UWB precision location system [2] can be used to identify and locate valuable assets in hospitals, industrial fields, government offices, etc. A UWB ASIC (application specific integrated circuit) device (low cost and small size) can be employed for recreational activities [3,4]. Another important/potential application is in sensor networks. Awareness of sensor positions may effectively improve network performance. For instance, location-aware routing protocols can reduce routing overhead and save energy by avoiding route search [5]. UWB technology is particularly well suited for sensor network applications due to its low power consumption.

This chapter aims to provide a comprehensive and detailed view over the localization techniques. It also provides an opportunity for the authors to present their research results.

2 Time-of-Arrival Estimation

Positioning techniques exploit one or more characteristics of radio signals to estimate the position of their sources. Some of the parameters that have been traditionally used for positioning are the received signal strength intensity (RSSI), the angle of arrival (AOA) and time of arrival (TOA). Amongst these positioning parameters, the RSSI is the least adequate for the UWB case, since it does not profit from

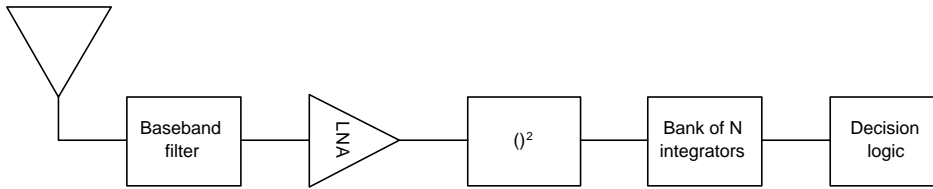


Figure 1: Block diagram of the non-coherent (energy collection) receiver.

the fine space-time resolution of impulsive signals and requires a site-specific path loss model [6]. The estimation of AOA, on the other hand, requires multiple antennas (or at least an antenna capable of beamforming) at the receiver. This requirement implies size and complexity requirements that are often not compatible with the low-cost, small-size constraints associated with applications such as wireless sensor networks which UWB technology is particularly suited for.

One of the most attracting characteristics of IR-UWB signals is the fine time resolution, which makes impulse-based UWB a prominent candidate technology for indoor positioning. Therefore, TOA stands out as the most suitable signal parameter to be used for positioning with UWB devices. However, due to the ultra short (usually sub nanoseconds) pulses, it poses challenges for synchronization in UWB systems. Some techniques have been proposed to estimate the TOA of UWB signals, for instance, correlation in conjunction with serial search [7], special code design [8], and frequency-domain processing [9]. All the above solutions seem, however, to be in conflict with the strict requirements of low cost and low complexity imposed on some UWB applications and may not provide satisfactory TOA estimate. Another TOA estimation scheme for UWB signal is the generalized likelihood ratio test [10] that seems to be high hardware complexity demanding.

In order to further reduce the complexity of UWB systems, non-coherent receivers such as energy collection [11–13] and transmitted reference based [14–17] have been recently proposed. Since energy collection based approach is promising and practical, we will first give this approach some detailed descriptions. Then, a two-stage TOA estimation scheme will be presented.

2.1 Energy-Collection Based TOA estimation

Figure 1 shows the block diagram of the energy detection receiver. The received signal is first passed through a band pass filter (BPF) to reduce the noise power. After low noise amplification, the signal is squared and then passed to a block of integrators that integrate the received signal in different time slots. The advantage of this receiver scheme is essentially represented by the relatively easy implementation when compared with the correlation based scheme. The drawback of the non-coherent approach is the noise enhancement due to the squaring and the reduced time resolution that is proportional to the length of the integration.

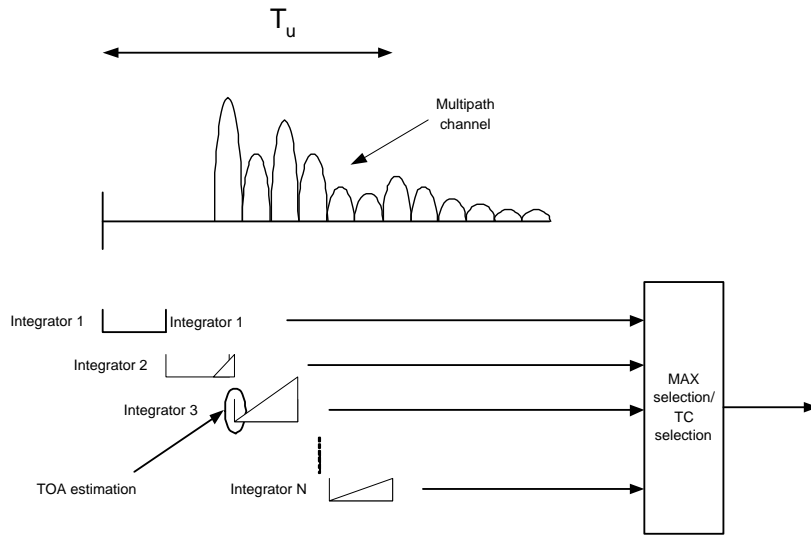


Figure 2: Illustration of MAX algorithm.

In order to reuse the same receiver architecture, TOA estimation can also be performed based on energy detection. After initial synchronization is completed, the TOA estimation is performed by dividing the uncertainty region (T_u) around the synchronization point in N integration windows, where N represents the number of integrators available in the receiver. Intuitively the estimation accuracy is dependent on the uncertainty region size and on the number of integrators. Differently from synchronization, which provides the time reference that insures the maximum signal energy detection, the TOA estimation can be seen as fine synchronization, searching for the arrival time of the received signal.

Based on the energy measurements, a decision is made according to a chosen criterion. In the hypothesis testing (decision making), three basic criteria may be considered. The first is the threshold crossing (TC) criterion. With TC, the search is performed serially and is stopped once a measurement value crosses the threshold. The corresponding integrator is then chosen and its switch-on time provides the TOA information. If necessary, a verification process may be pursued. In the event that no measurement crosses the threshold, new measurements are taken and the search resumes. The TC algorithm requires the setting of a threshold.

The other approach is the maximum selection (MAX) criterion. With this criterion, measurements at all sectors are first compared. Then, the maximal measurement is produced and the relevant window is selected. In the event that no appropriate thresholds can be readily obtained, the MAX criterion could be desirable. Figure 2 shows the basic principle of the MAX algorithm with the switch-on time of integrator 3 chosen to be the TOA estimate. Another criterion is the hybrid of MAX and TC. In this hybrid criterion, the maximal measurement is first obtained. Then, the maximum is examined against the threshold. If the threshold is crossed, the related integration window is selected. If the maximum does not cross the threshold, the search resumes.

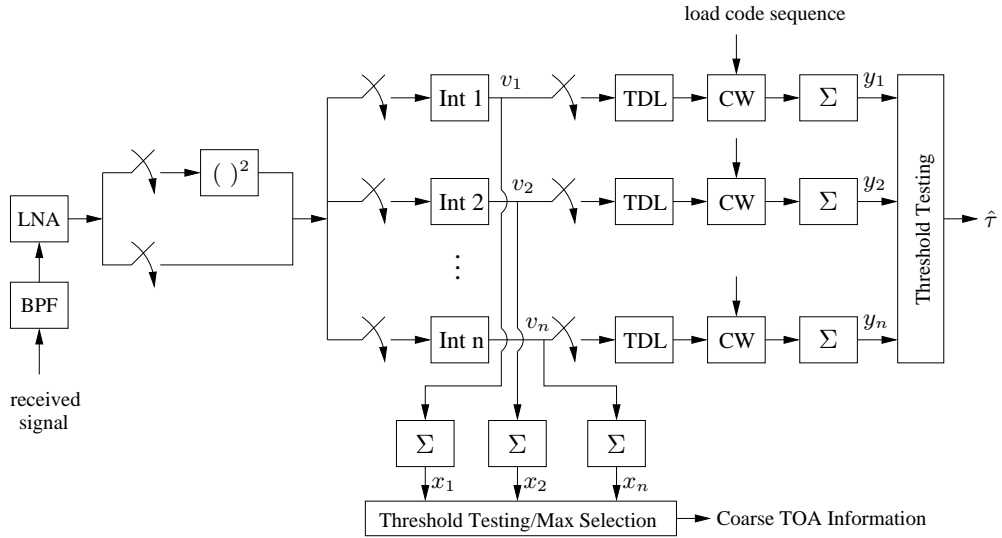


Figure 3: Acquisition system structure. BPF: bandpass filter. LNA: low noise amplifier. Int: integrator. TDL: tapped delay line. CW: code weighting.

2.2 Two-Stage TOA Estimation

The above discussed energy collection based approach is low-complexity and easy to implement, however, it may not provide satisfactory TOA estimation performance for high accuracy demanding systems. For low data rate communications, it is desirable to achieve fast synchronization or TOA estimation. In this section, we study a two-stage TOA estimation scheme [18] to achieve the goal of rapid acquisition and high accuracy.

2.2.1 First Stage Processing

In the preamble of the packet, there are a sequence of symbols assigned for synchronization, each of which consists of a sequence of coded pulses of length T_{ps} which is a small fraction of the symbol period. During the first stage, a search is performed over a duration of one or more symbols. The symbol duration is divided into K sectors of equal size of $T_{sect} = T/K$. The aim is to determine which sector will contain the pulses. Then code acquisition can be rapidly achieved at the second stage. Fig. 3 shows the block diagram of the proposed acquisition system.

After passing through a bandpass filter and a low noise amplifier, the received signal is squared and then forwarded to a bank of n integrators as shown in Fig. 3. The first integrator starts integration at a chosen time instant. Each of the other integrators switches on once its preceding integrator switches off. The integration interval of each integrator is the same and equal to the sector size T_{sect} . The process is similar to the technique employed in the previous section. It may go over κ symbols and the energy measurements at the same sector are accumulated.

Once the energy measurements are available, a decision is made according to one of the three criteria. When the TC is applied, a decision is made by choosing one of the two hypotheses:

- $\mathcal{H}_{1,0}$: no signal pulses appear in the sector examined,
- $\mathcal{H}_{1,1}$: at least one signal pulse appears in the sector examined.

Then, two types of errors can be made when making a decision:

- decide $\mathcal{H}_{1,1}$ when $\mathcal{H}_{1,0}$ is true and the corresponding probability is denoted by $P(\mathcal{H}_{1,1}; \mathcal{H}_{1,0})$,
- decide $\mathcal{H}_{1,0}$ when $\mathcal{H}_{1,1}$ is true and the probability is denoted by $P(\mathcal{H}_{1,0}; \mathcal{H}_{1,1})$.

Similarly to the terminologies used in code acquisition, $P(\mathcal{H}_{1,1}; \mathcal{H}_{1,0})$ is termed the probability of false alarm and is denoted by P_{F1} . The probability, $P(\mathcal{H}_{1,1}; \mathcal{H}_{1,1})$, is termed the probability of detection, which is denoted by P_{D1} . The probability of missing is the probability that all measurements are less than the threshold.

According to the Neyman-Pearson theorem [19], for a given $P_{F1} = \alpha_1$, P_{D1} is maximized by deciding $\mathcal{H}_{1,1}$ if

$$L(x_i) = p(x_i; \mathcal{H}_{1,1})/p(x_i; \mathcal{H}_{1,0}) > \gamma_0$$

where $p(x_i; \mathcal{H}_{1,j})$, $j = 1$ and 2 , is the probability density function (pdf) and the threshold γ_0 is found from

$$P_{F1} = \int_{x_i; L(x_i) > \gamma_0} p(x_i; \mathcal{H}_{1,0}) dx_i = \alpha_1$$

Here x_i is the energy measurement. Suppose that there are L_{sect} samples in each sector and κ measurements are accumulated. When no signal pulses appear, $x_i = \sum_{j=1}^{\kappa L_{sect}} z_j^2$ where z_j is a Gaussian random variable of mean zero and variance σ^2 , has a chi-square (or gamma) distribution [20] with pdf

$$p(x) = \frac{1}{(2\sigma^2)^{m_1/2} \Gamma(m_1/2)} x^{m_1/2-1} \exp\left(-\frac{x}{2\sigma^2}\right)$$

where $m_1 = \kappa L_{sect}$. Without loss of generality, let m_1 be even: $m_1 = 2m$ and the solution of $L(x_i) > \gamma_0$ is $x_i > \gamma_1$. Then, the false alarm can be expressed by

$$P_{F1} = \int_{\gamma_1}^{\infty} p(x) dx = \exp\left(-\frac{\gamma_1}{2\sigma^2}\right) \sum_{k=0}^{m-1} \frac{1}{k!} \left(\frac{\gamma_1}{2\sigma^2}\right)^k$$

Since there are many cases when at least one signal pulse appears in a sector of interest, it would be impractical to derive a tractable expression for the probability of detection (as well as the probability of missing) even when the multipath channel information is available. This also happens to the probabilities when either the MSC or the hybrid criterion is employed.

For clarity, we assume that the first symbol of the received signal is among the symbol(s) examined. We also assume that the i -th sector is chosen and it was switched on at t_i . In a probability dependant

on the SNR, some pulses of the received signal will be locked in the i -th sector and the TOA would be at some point around t_i . Therefore, at the second (code acquisition) stage, we may constrain the TOA to:

$$t_i - (T_{ps} + T_m) < t < t_i + T_{sect} \quad (1)$$

where T_m is the multipath spread which may be in usual unknown; however, it may be roughly predicted based on the channel condition, if available. The goal of the first stage is to lock the pulse sequence in the region given by (1). Therefore, the probability that the pulse sequence is not locked in the region is one of the key indices to measure the performance at the first stage. We call this probability as the probability of unlocking, denoted by P_{UL} .

2.2.2 Second Stage Processing

In the second stage, i.e. the code acquisition stage, the received signal is passed directly to the integrators which now become part of the matched filter correlator (consisting of the integrator, the tapped delay line (TDL), the code weighting (CW), and the summation) [21, 22]. The located region given by (1) is divided into a group of cells.

The MAX and the hybrid criterion may not be appropriate for the second stage due to the multipath channels, so that the threshold crossing criterion is exploited. The correlations (y_1 to y_n in Fig. 3) are examined serially. Once the correlation of a cell crosses the threshold, it is selected as the correct cell whose time instant becomes the TOA estimate. Similarly to the technique at the first stage, correlations of the same code offset can be produced over several symbols and then be accumulated to increase the accuracy.

For an L -path channel, there are $(L+1)$ hypotheses denoted by $\mathcal{H}_{2,0}$: no signal appears, and $\mathcal{H}_{2,i}$, $i = 1, 2, \dots, L$: i -th path signal appears. Since the signal of the first path is of interest, only two decisions will be made, i.e. $\mathcal{H}_{2,1}$ is true or not. If $\mathcal{H}_{2,0}$ is true and assume that κ_2 measurements are accumulated, the correlation has a Gaussian distribution of mean zero and variance $\sigma_2^2 = \kappa_2 m_s \sigma^2$ where m_s is the code length. Let P_{F2} denote the probability of false alarm at the second stage, which is the probability of deciding $\mathcal{H}_{2,1}$ when $\mathcal{H}_{2,0}$ is true. Then,

$$P_{F2} = \int_{\gamma_2}^{\infty} \frac{1}{\sqrt{2\pi}\sigma_2} \exp\left[-\frac{x^2}{2\sigma_2^2}\right] dx \quad (2)$$

where γ_2 is the threshold at the second stage. Denote P_{D2} be the probability of detection at the second stage, which is also channel-dependent. Then, when $\mathcal{H}_{2,1}$ is true, we have

$$P_{D2} = \int_{\gamma_2}^{\infty} \frac{1}{\sqrt{2\pi}\sigma_2} \exp\left(-\frac{(x - \kappa_2 a_0)^2}{2\sigma_2^2}\right) dx$$

where a_0 is the constant amplitude of the first path signal.

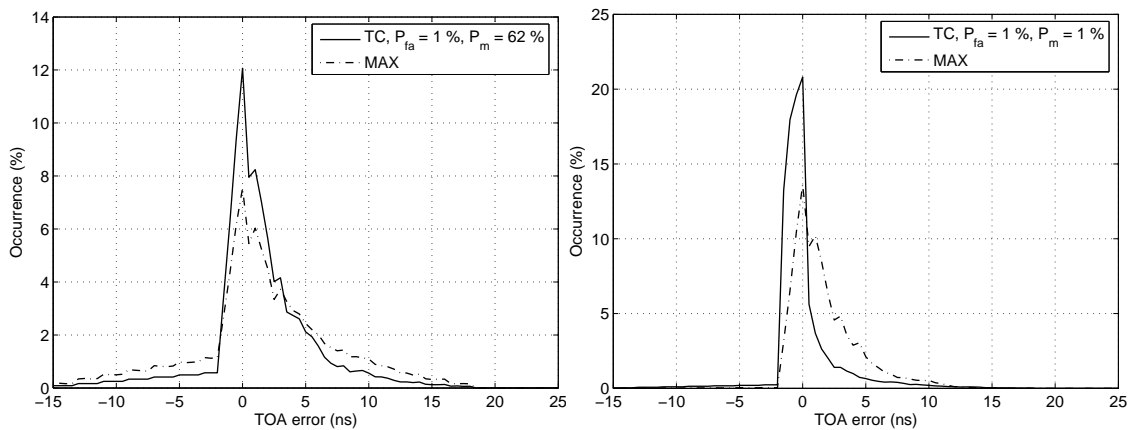


Figure 4: Comparison between MAX and TC algorithm. $T_u = 15$ ns, $N = 10$, $T_{int} = 2$ ns and $E_b/N_0 = 10$ dB (left) and $E_b/N_0 = 20$ dB (right).

2.3 Simulation Results

This subsection presents some simulation results of the energy-collection based approach. In the case of LOS or non-sever NLOS propagation, the channel is characterized by the presence of the high bunch of energy in the first nanoseconds of the received signal. In this case the MAX algorithm can achieve the same performance of the TC but with much less implementation issues and with negligible probability of miss-detection. Figure 4 shows the performance of the two proposed algorithms. These results are obtained by employing the channel model 3 (CM3) as defined by the 802.15.4a standardization group using 1000 channel realizations. The TC algorithm tends to outperform the MAX algorithm, however, at low signal-to-noise ratio (SNR), the probability of miss-detection (P_m) can considerably increase. In these specific cases the threshold is set based on the probability of false alarm (P_{fa}) estimated over a number of integrated noise signal values. Adaptive threshold based on the received signal strength might reduce the probability of miss detection, however, the SNR estimation of UWB signal is not an easy task and it may not be suited for low complexity devices. Another option to reduce the probability of miss-detection is to increase the integration window to increase the received signal strength.

3 Location and Tracking

In this section, an overview of position estimation algorithms of both non-iterative and iterative is provided and details of several typical algorithms are presented. Also presented are mobile node/station tracking and mobile track smoothing. The block diagram of the location and tracking system is illustrated in Figure 5

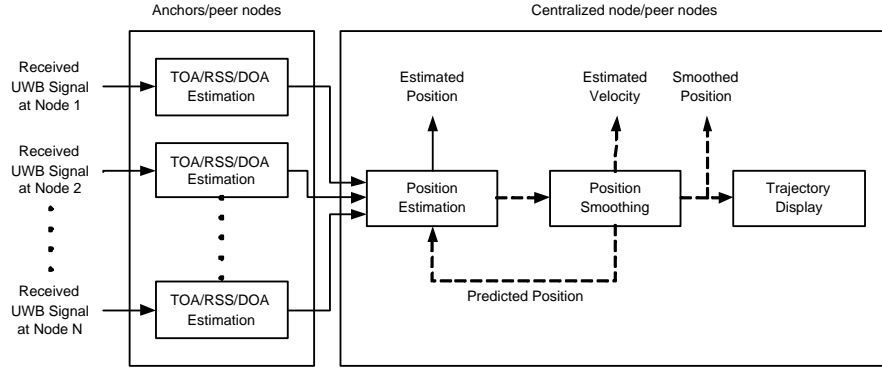


Figure 5: Block diagram of position location and tracking.

3.1 Position Estimation

When radio signal including UWB signal is employed¹, position estimation algorithms may be broken into two broad categories: iterative and non-iterative methods, for both cellular systems and sensor networks.

3.1.1 Non-Iterative Algorithms

A variety of non-iterative algorithms have been developed for position estimation. The most straightforward one is the direct method [23, 24] which directly solves a set of simultaneous equations with four anchors for 3-D positioning using TDOA measurements. This method, however, may not effectively exploit extra measurements from extra sensors to improve position accuracy. The spherical-interpolation (SI) method [25] and related approaches [26, 27] were developed to exploit extra measurements. To approach optimal estimation, the two-stage maximum likelihood approach was considered in [28] and the linear-correction least square approach was considered in [29]. When using range measurements, the standard least-squares (LS) approach is commonly considered [30–32]. For quick reference, the LS and the SI approaches are described as follows. For convenience, we assume that the nodes with known positions, (x_i, y_i, z_i) , $i = 1, 2, \dots, N$, are anchors while the nodes with unknown positions, (x, y, z) , are sensors.

Let t_i be the TOA of the signal at anchor i , t_0 be the transmit time at the sensor, c be the speed of light, and $d_i = c(t_i - t_0)$ be the range between the sensor and the i -th anchor. Then, we obtain

$$d_i = \sqrt{(x_i - x)^2 + (y_i - y)^2 + (z_i - z)^2}, \quad i = 1, 2, \dots, N. \quad (3)$$

Squaring both sides of (3) yields

$$(x_i - x)^2 + (y_i - y)^2 + (z_i - z)^2 = d_i^2. \quad (4)$$

¹Several parameters of the received signal have been commonly exploited: TOA (and thus time-difference-of-arrival (TDOA) and round trip time (RTT)), received signal strength (RSS), and angle of arrival (AOA).

Subtracting (4) for $i = 2, 3, \dots, N$ by (4) for $i = 1$ produces

$$x_{i,1}x + y_{i,1}y + z_{i,1}z = g_{i,1}, \quad i = 2, \dots, N \quad (5)$$

where

$$\begin{aligned} x_{i,1} &= x_i - x_1, & y_{i,1} &= y_i - y_1, & z_{i,1} &= z_i - z_1, \\ g_{i,1} &= 0.5 [(x_i^2 + y_i^2 + z_i^2) - (x_1^2 + y_1^2 + z_1^2) + d_1^2 - d_i^2] \end{aligned}$$

Equation (5) can be written in compact form as

$$\mathbf{A}\mathbf{p} = \mathbf{b} \quad (6)$$

where

$$\mathbf{A} = \begin{bmatrix} x_{2,1} & y_{2,1} & z_{2,1} \\ x_{3,1} & y_{3,1} & z_{3,1} \\ \vdots & \vdots & \vdots \\ x_{N,1} & y_{N,1} & z_{N,1} \end{bmatrix}, \quad \mathbf{p} = \begin{bmatrix} x \\ y \\ z \end{bmatrix}, \quad \mathbf{b} = \begin{bmatrix} g_{2,1} \\ g_{3,1} \\ \vdots \\ g_{N,1} \end{bmatrix}. \quad (7)$$

The standard LS solution to (6) is given by

$$\hat{\mathbf{p}} = (\mathbf{A}^T \mathbf{A})^{-1} \mathbf{A}^T \mathbf{b} \quad (8)$$

where the matrix inverse is supposed to exist and d_i are replaced by their corresponding estimates.

When the transmit time t_0 is unknown, TDOA measurements can be employed as for centralized networks. In this case, the SI method would be a suitable candidate. First map the spatial origin to one of the anchors, say anchor 1, as shown in Fig. 6. Define

$$R_i = \sqrt{x_i^2 + y_i^2 + z_i^2}, \quad \mathbf{p}_i = [x_i, y_i, z_i]^T, \quad R = \sqrt{x^2 + y^2 + z^2}, \quad d_{i,j} = d_i - d_j.$$

Then, from the Pythagorean theorem, we have

$$(R + d_{i,1})^2 = R_i^2 - 2\mathbf{p}_i^T \mathbf{p} + R^2, \quad i = 2, 3, \dots, N. \quad (9)$$

In the presence of measurement errors, (9) becomes

$$\epsilon_i = R_i^2 - d_{i,1}^2 - 2Rd_{i,1} - 2\mathbf{p}_i^T \mathbf{p} \quad (10)$$

where ϵ_i is the equation error. Equation (10) can be written in compact form as

$$\boldsymbol{\epsilon} = \boldsymbol{\delta} - 2R\mathbf{d} - 2\mathbf{A}\mathbf{p} \quad (11)$$

where \mathbf{A} is given by (6), $\boldsymbol{\epsilon}$ is the equation error vector, and

$$\boldsymbol{\delta} = [R_2^2 - d_{2,1}^2, R_3^2 - d_{3,1}^2, \dots, R_N^2 - d_{N,1}^2]^T, \quad \mathbf{d} = [d_{2,1}, d_{3,1}, \dots, d_{N,1}]^T.$$

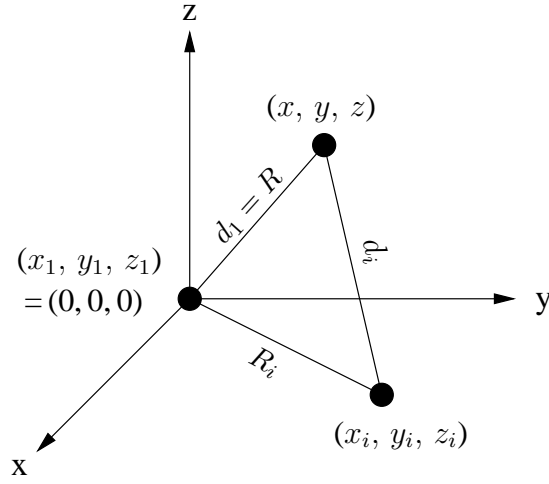


Figure 6: Illustration for spherical interpolation approach.

The standard LS solution for \mathbf{p} , given R , is

$$\mathbf{p} = \frac{1}{2} (\mathbf{A}^T \mathbf{A})^{-1} \mathbf{A}^T (\boldsymbol{\delta} - 2R\mathbf{d}) \quad (12)$$

The key idea of the SI approach is to substitute (12) into (11) and minimize the equation error again but with respect to R . The source location estimate is then obtained as

$$\hat{\mathbf{p}} = \frac{1}{2} (\mathbf{A}^T \mathbf{W} \mathbf{A})^{-1} \mathbf{A}^T \mathbf{W} \left(\mathbf{I} - \frac{\mathbf{d} \mathbf{d}^T \mathbf{B} \mathbf{V} \mathbf{B}}{\mathbf{d}^T \mathbf{B} \mathbf{V} \mathbf{B} \mathbf{d}} \right) \quad (13)$$

where \mathbf{W} and \mathbf{V} are weighting matrixes and

$$\mathbf{B} = \mathbf{I} - \mathbf{A} (\mathbf{A}^T \mathbf{W} \mathbf{A})^{-1} \mathbf{A}^T \mathbf{W}$$

3.1.2 Iterative Algorithms

For both cellular networks and sensor networks, two iterative methods are often considered. One is the Taylor series method [28, 33–37] and the other is the optimization based method [38–40].

In Taylor series method, a set of nonlinear equations is linearized by expanding it in a Taylor series around a point (initially an estimate of the actual position) and keeping only terms below second order. The set of linearized equations is solved to produce a new approximate position and the process continues until a pre-specified criterion is satisfied. When TDOA measurements are employed, this method may be described as follows.

Subtracting (3) for $i = 1$ from (3) for $i = 2, 3, \dots, N$ produces

$$\sqrt{(x - x_i)^2 + (y - y_i)^2 + (z - z_i)^2} - \sqrt{(x - x_1)^2 + (y - y_1)^2 + (z - z_1)^2} = c(t_i - t_1), \quad i = 2, 3, \dots, N. \quad (14)$$

Define

$$f_i(x, y, z) = \sqrt{(x - x_{i+1})^2 + (y - y_{i+1})^2 + (z - z_{i+1})^2} - \sqrt{(x - x_1)^2 + (y - y_1)^2 + (z - z_1)^2},$$

$$i = 1, 2, \dots, N - 1,$$

and let \hat{t}_i be the TOA estimate at anchor i . Then,

$$f_i(x, y, z) = \hat{d}_{i+1,1} + \epsilon_{i+1,1}, \quad i = 1, 2, \dots, N - 1,$$

where $\hat{d}_{i,1} = c(\hat{t}_i - \hat{t}_1)$ and $\epsilon_{i,1}$ is the corresponding range difference estimation error with covariance \mathbf{R} . If x_v, y_v , and z_v are guesses of the actual sensor position, then,

$$x = x_v + \delta_x, \quad y = y_v + \delta_y, \quad z = z_v + \delta_z$$

where δ_x, δ_y , and δ_z are the position errors to be determined. Expanding f_i in Taylor series and retaining the first two terms produce

$$f_{i,v} + a_{i,1}\delta_x + a_{i,2}\delta_y + a_{i,3}\delta_z \approx \hat{d}_{i+1,1} + \epsilon_{i+1,1}, \quad i = 1, 2, \dots, N - 1, \quad (15)$$

where

$$f_{i,v} = f_i(x_v, y_v, z_v)$$

$$a_{i,1} = \left. \frac{\partial f_i}{\partial x} \right|_{x_v, y_v, z_v} = \frac{x_1 - x_v}{\hat{d}_1} - \frac{x_{i+1} - x_v}{\hat{d}_{i+1}}, \quad \hat{d}_i = \sqrt{(x_v - x_i)^2 + (y_v - y_i)^2 + (z_v - z_i)^2}$$

$$a_{i,2} = \left. \frac{\partial f_i}{\partial y} \right|_{x_v, y_v, z_v} = \frac{y_1 - y_v}{\hat{d}_1} - \frac{y_{i+1} - y_v}{\hat{d}_{i+1}}, \quad a_{i,3} = \left. \frac{\partial f_i}{\partial z} \right|_{x_v, y_v, z_v} = \frac{z_1 - z_v}{\hat{d}_1} - \frac{z_{i+1} - z_v}{\hat{d}_{i+1}} \quad (16)$$

Equation (15) can be rewritten as

$$\mathbf{A}\boldsymbol{\delta} = \mathbf{D} + \mathbf{e} \quad (17)$$

where

$$\mathbf{A} = \begin{bmatrix} a_{1,1} & a_{1,2} & a_{1,3} \\ a_{2,1} & a_{2,2} & a_{2,3} \\ \vdots & \vdots & \vdots \\ a_{N-1,1} & a_{N-1,2} & a_{N-1,3} \end{bmatrix}, \quad \boldsymbol{\delta} = \begin{bmatrix} \delta_x \\ \delta_y \\ \delta_z \end{bmatrix}$$

$$\mathbf{D} = \begin{bmatrix} \hat{d}_{2,1} - f_{1,v} \\ \hat{d}_{3,1} - f_{2,v} \\ \vdots \\ \hat{d}_{N,1} - f_{N-1,v} \end{bmatrix}, \quad \mathbf{e} = \begin{bmatrix} \epsilon_{2,1} \\ \epsilon_{3,1} \\ \vdots \\ \epsilon_{N,1} \end{bmatrix}$$

The weighted least-square estimator for (17) produces

$$\boldsymbol{\delta} = [\mathbf{A}^T \mathbf{R}^{-1} \mathbf{A}]^{-1} \mathbf{A}^T \mathbf{R}^{-1} \mathbf{D} \quad (18)$$

Given an initial position guess (x_v, y_v, z_v) and compute δ with (18). Then update the position estimate according to

$$x_v = x_v + \delta_x, \quad y_v = y_v + \delta_y, \quad z_v = z_v + \delta_z.$$

Continually refine the position estimate until δ is sufficiently small. In some cases, the convergence of Taylor series method may not be satisfactory. To improve the convergence of this method, a modified Taylor series method has been proposed in [18]. Compared to the original method, the convergence of the modified scheme is considerably increased under a variety of scenarios.

In optimization based approaches, an objective/cost function is first defined. One such cost function may be chosen to be

$$\epsilon = \sum_{i=1}^N \left[\sqrt{(x_i - x)^2 + (y_i - y)^2 + (z_i - z)^2} - c(t_i - t_0) \right]^2 \quad (19)$$

Then, a minimization algorithm is applied to achieve the optimal solution to the position estimation. Both unconstrained and constrained minimization algorithms can be employed [41]. The Quasi-Newton DFP algorithm was exploited in the UWB precision assets location system [2]. A Gauss-Newton type Levenberg-Marquardt method [42] was studied in [43]. Convex optimization was considered in [44] and the simplex method [45] was employed in [46]. The above mentioned algorithms can be found in the Matlab optimization toolbox.

3.2 Tracking

We consider a scenario where the sensor nodes are mobile. To make use of accurate node position information for efficient network operation and management, node position information needs to be updated regularly. The updating frequency should be based on the mobility/speed of the nodes of interest. Suppose that the maximum moving speed of the nodes in the desired sensor network is 18 km/hr (that is 5 meters per second). If the position error is required to be below one meter, we need to update the position information at least 5 times per second. Higher position accuracy requirement will require higher updating rate. Different updating frequency may be applied to different nodes if the maximum velocity of the nodes is different and they are known a priori. This strategy would improve the network efficiency.

Positioning performance can be further improved by smoothing the tracks of the moving nodes. Smoothing techniques including Kalman filtering [4, 47, 48] and linear least square technique [4, 49] can be employed.

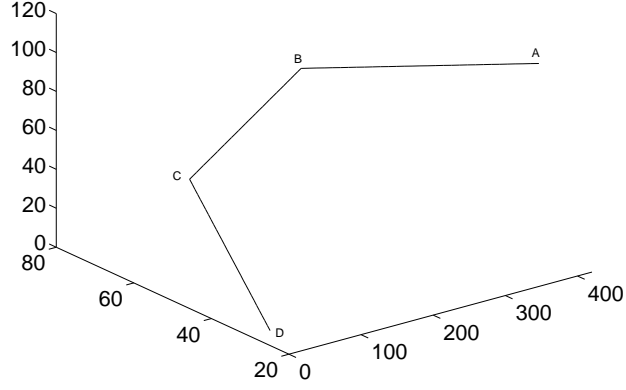


Figure 7: Track for examination.

No of FNs	4	5	6	8
DFP	4.36 (m)	1.65 (m)	0.63 (m)	0.15 (m)
TS	5.43	2.1	0.88	0.15
SI		1.55	0.33	0.09
DM	7.54			

Table 1: Averaged RMSEs of four algorithms at SNR of 16 dB. FNs: fixed nodes. TS: Taylor-series method. SI: spherical-interpolation method. DM: direct method.

3.3 Simulation Results

In this section, we examine the performance of location and tracking. We use one of the realistic field structures, a snow covered slope of dimensions about $400\text{m} \times 100\text{m} \times 100\text{m}$ [4]. The anchor nodes will be deployed along both sides of the slope and mounted on poles of varying height. Fig. 7 shows the track for examination. The skier moves from A to B (120 m) at a speed of 8 meters per second (m/s). The skier moves from B to C (160m) at a speed of 10 m/s and finally from C to D (120 m) at a speed of 8 m/s.

First we examine the performance of the different position estimation algorithms under the more realistic circumstance. Two hundred different combinations of fixed node positions are tested and then the results are averaged. Tables 1 and 2 compare the averaged results of the four algorithms at SNR of 16 dB

For the parameters examined, the spherical-interpolation method provides the best tradeoff between performance and complexity when there are at least five fixed nodes. To achieve sub-meter accuracy, at least six fixed nodes are needed with SNR up to 16 dB.

No of FNs	4	5	6	8
DFP	10.8 (%)	6.6 (%)	5.2 (%)	4.2 (%)
TS	14.3	3.1	1.5	0.9
SI		3.4	1.3	0.9
DM	46.6			

Table 2: Averaged Failure Rates of four algorithms at SNR of 16 dB.

before smoothing	LS	KF
4.13 (m)	2.40	2.30
2.70 (m)	1.58	1.30
1.40 (m)	1.02	0.99

Table 3: Averaged RMSEs before and after smoothing. KF: Kalman filtering.

Let us consider position smoothing by making use of Kalman filtering and the LS method. Table 3 shows the averaged RMSEs before and after smoothing. The estimated tracks (before smoothing) are produced by using the SI algorithm with five fixed nodes under three sets of fixed node configurations. Although Kalman filtering performs better, the performance gain is marginal compared to the increase in complexity.

4 Location in Distributed Architectures

In this section, we consider localization in ad-hoc and distributed networks. An ad-hoc network is a collection of wireless nodes that self-configure themselves to form a network without the aid of any infrastructure. This sort of networks are characterized by large size, need for distributed coordination and ubiquitous connectivity, power constraints and the ability to be ad hoc deployable. In the following subsections, an overview of related localization approaches is first presented. Then a positioning algorithm is proposed and finally some simulation results are provided.

4.1 Overview

In the recent years, there have been numerous algorithms (either centralized or distributed) to localize sensor nodes in wireless sensor networks. In [44, 50], a centralized scheme is proposed which collects the entire topology in a server to minimize the errors using convex optimization. In [51–53], instead of directly solving the set of constraints of the whole wireless network, multi dimensional scaling (MDS) is exploited. This technique uses local connectivity or distance measure to generate relative maps that

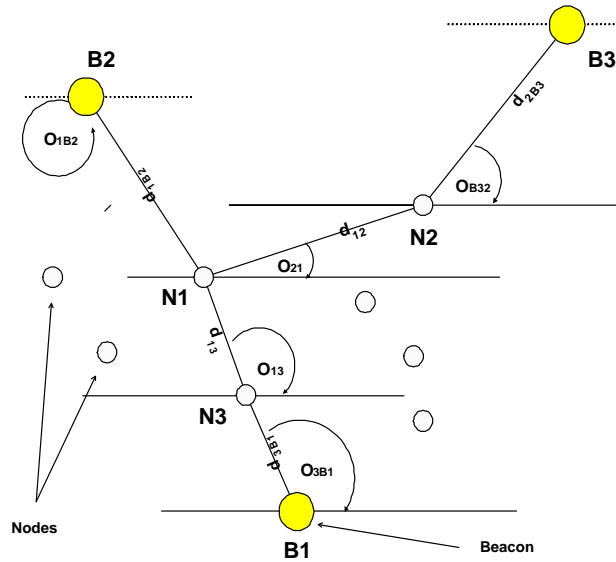


Figure 8: Scheme of Wireless Sensor Network

represent the relative position of nodes. The main problem of the mentioned algorithms is the need to have some powerful node or server to perform the large computation. In [54], distributed algorithms are divided in two sub-families: range-based and range-free algorithms. In range-free localization [30, 55], beacon nodes broadcast their positions to their neighbors that keep an account of all received beacons. Then, nodes calculate their positions based on the received beacon locations, the hop-count from the corresponding beacon and the average distance per hop. In [56], the distance per hop is averaged by taking into account the local density of nodes. In range-based algorithms, the distance between two neighboring sensors is first estimated, for example, by using TOA measurements. In [57] and more recently in [58], a distributed mechanism is proposed for GPS-free positioning in mobile ad-hoc networks. A slightly modified version of the GPS-free algorithm is proposed in [59]. In [60], the distance between a sensor and a beacon is directly calculated using basic triangle rules and simple geometry. Collinearity is exploited in [61] and factor graphs are employed in [62].

4.2 Proposed Algorithm

It is assumed that each node (sensor node and beacon node) has the ability of measuring both TOA and AOA with its 1-hop neighbors. In the first phase, the beacons broadcast their coordinates. Then, all nodes establish the shortest path with the beacons. As a result, a node should have the coordinates of at least three beacons and the path to reach them. After the shortest path is developed, all nodes belonging to the path calculate the TOA and AOA with the neighboring nodes in the path. Then, using the TOA and AOA measurements, a node is able to estimate the Euclidean distance to each of at least 3 beacons.

Figure 4.2 gives an illustration of the algorithm. In the figure, node N1 established a path to each of

the three beacons (B1, B2 and B3). Then, it stores the relevant information in its data base in the form

$$\begin{aligned}
N_1 \rightarrow B_1 : & \quad \Phi_1 = \{(N_1, N_3, B_1), (\hat{O}_{13}, \hat{O}_{3B_1}), (\hat{d}_{13}, \hat{d}_{3B_1})\} \\
N_1 \rightarrow B_2 : & \quad \Phi_2 = \{(N_1, B_2), (\hat{O}_{1B_2}), (\hat{d}_{1B_2})\} \\
N_1 \rightarrow B_3 : & \quad \Phi_3 = \{(N_1, N_2, B_3), (\hat{O}_{21}, \hat{O}_{B_32}), (\hat{d}_{12}, \hat{d}_{2B_3})\}
\end{aligned}$$

After obtaining the distance to each of the beacons, the position coordinates of the node can be estimated using the algorithms studied in section 3. When considering the optimization based approaches, the cost function is defined as

$$\epsilon(X, Y) = \sum_{k=1}^{N_B} \left[\sqrt{\left(\sum_{i=1}^{N_{hop}(k)} \hat{d}_i \cos(\hat{\alpha}_i) \right)^2 + \left(\sum_{i=1}^{N_{hop}(k)} \hat{d}_i \sin(\hat{\alpha}_i) \right)^2} - \sqrt{(X_k - X)^2 + (Y_k - Y)^2} \right]^2 \quad (20)$$

Where $\hat{\alpha}_i$ and \hat{d}_i are respectively the estimated angle and the estimated distance between two neighboring nodes belonging to the path, N_B is the number of beacons available in the network, and $N_{hop}(k)$ is the number of hops between the node and a given beacon. Although we focused on 2-D node location, it is straightforward to extend the algorithm to 3-D positioning.

4.3 Simulations Results

The monitored area has dimensions of $100(w) \times 100(l)$ m. 100 nodes are randomly positioned in the area together with a number (5, 15, and 20) of beacon nodes depending on the simulation scenarios. The transmission radius of any node in this network is equal to 30 m and it is kept constant. The positioning algorithms considered are the DFP algorithm and the direct method (DM). The performance evaluation is performed by assuming that the TOA and AOA measurement errors are white Gaussian random variables of mean zero and variance σ_{TOA}^2 and σ_{AOA}^2 , respectively. At each test point (σ), 30 simulations are conducted with new random topology of the network and the performance is then averaged. In the case of the DFP algorithm, 50 iterations are used to update the estimated coordinates.

Figure 9 shows the root mean square error of the coordinates estimations using either the DM or DFP algorithm. In general, the RMS errors of both algorithms are under two meters and the DFP algorithm results in higher accuracy. We also notice the quite flat curve (except for the case of DM with $\sigma_{TOA} = 0$) as the AOA measurements error increases. It means that the algorithms, to localize the nodes, are not sensitive to the AOA measurement error.

Figure 10 shows the RMS error with respect to σ_{TOA} at a given σ_{AOA} . In this case, the slope of the curves becomes sharper. This phenomena tells the fact that the algorithms are more sensitive to TOA measurement error, comparatively.

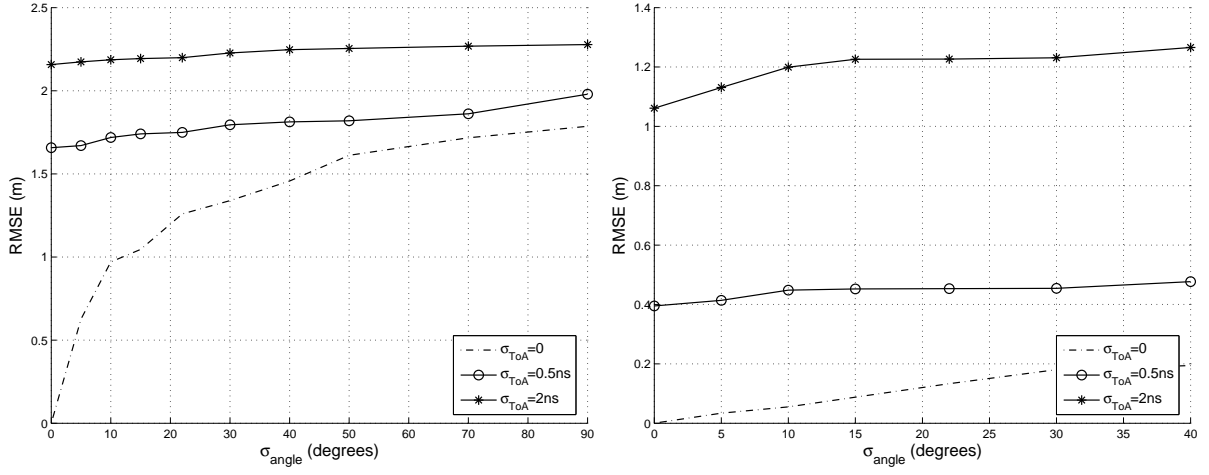


Figure 9: RMSE of direct method (left) and DFP algorithm (right) with respect to AOA errors. 5 beacons in the network and three different variances of the TOA error ($\sigma_{\text{TOA}} = \{0, 0.6, 2\}\text{ns}$).

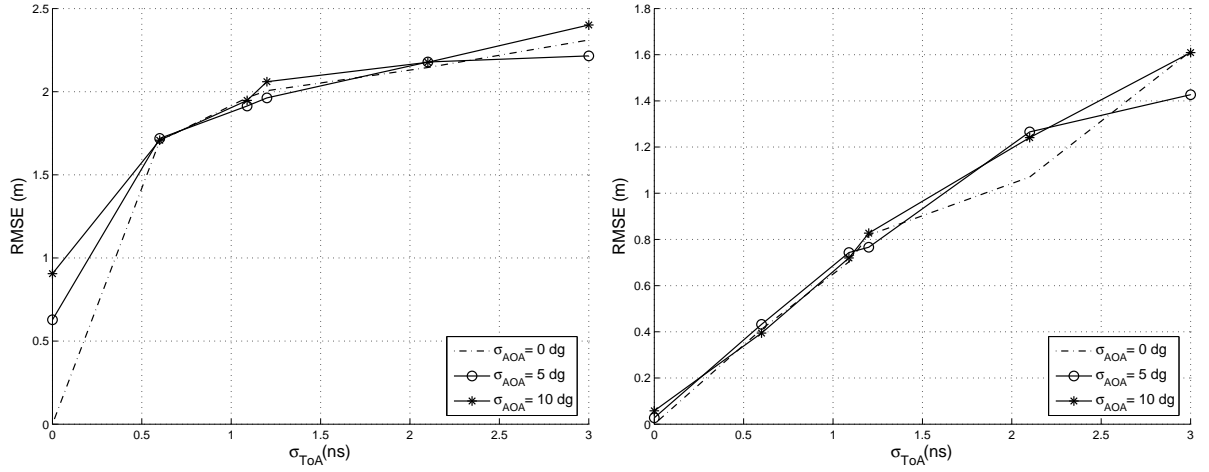


Figure 10: RMSE of direct method (left) and DFP algorithm (right) with respect to TOA errors. 5 beacons in the network and three different variances of the AOA error ($\sigma_{\text{AOA}} = \{0, 5, 10\}$ degrees).

Figure 11 shows the performance of the proposed algorithm when increasing the number of beacons. In general, it has been shown in some studies [24] that the higher the number of beacons is, the less the RMSE value is in centralized networks. Figure 11 confirms this result.

5 Theoretical Positioning Accuracy

The accuracy of a positioning method is dependent on several issues. The location accuracy with respect to measurement errors has been widely studied [33, 34, 63]. However, the effects of systematic errors have not been widely considered. Systematic errors include such factors as errors in known sensor locations and network synchronization. A tool to analyze the systematic errors is presented

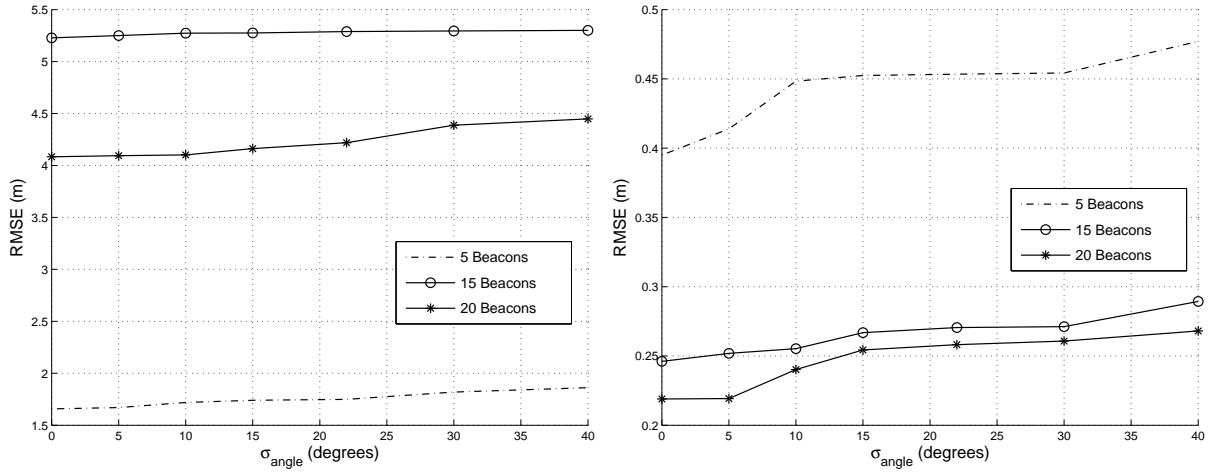


Figure 11: RMSE of direct method (left) and DFP algorithm (right) using 5, 15 and 20 beacons with $\sigma_{TOA} = 0.5$ ns.

in [34], but analysis is not performed therein. This method is closely related to error propagation laws²[64]. In this section we briefly explain this tool and apply it to analysis of the location accuracy of hyperbolic (time delay based) location system.

5.1 Analysis Tool

Let \mathbf{x} be the estimator of the actual location \mathbf{x}^0 either in two or three dimensions. The bias is $\mathbf{b} = E\{\mathbf{x} - \mathbf{x}^0\}$, the covariance $\mathbf{C} = E\{(\mathbf{x} - E\{\mathbf{x}\})(\mathbf{x} - E\{\mathbf{x}\})^T\}$, and the total mean squared error $\mathbf{V} = E\{(\mathbf{x} - \mathbf{x}^0)(\mathbf{x} - \mathbf{x}^0)^T\} = \mathbf{b}\mathbf{b}^T + \mathbf{C}$. Therefore, the analysis of the bias and covariance suffices to determine the accuracy of location systems.

Let the measurements without uncertainties be defined as $r_i^0 = f_i(\mathbf{x}^0, \mathbf{q}^0)$, or in a vector form

$$\mathbf{r}^0 = \mathbf{f}(\mathbf{x}^0, \mathbf{q}^0), \quad (21)$$

where \mathbf{q} , in general, denotes the system parameters that affect to the measurement model and \mathbf{q}^0 denotes the actual system parameters. The model is, in general, nonlinear. Therefore, it is linearized using the first two terms of the Taylor series of $\mathbf{r} = \mathbf{f}(\mathbf{x}, \mathbf{q})$ around \mathbf{x}^0 and \mathbf{q}^0 . It follows that

$$\mathbf{r} \approx \mathbf{f}(\mathbf{x}^0, \mathbf{q}^0) + J_{\mathbf{x}}(\mathbf{x}^0, \mathbf{q}^0)(\mathbf{x} - \mathbf{x}^0) + J_{\mathbf{q}}(\mathbf{x}^0, \mathbf{q}^0)(\mathbf{q} - \mathbf{q}^0), \quad (22)$$

where $J_{\mathbf{x}}(\mathbf{x}, \mathbf{z})$ and $J_{\mathbf{q}}(\mathbf{x}, \mathbf{q})$ are the Jacobians of $\mathbf{f}(\mathbf{x}, \mathbf{q})$ with respect to \mathbf{x} and \mathbf{q} . Solving this linear equation for $\mathbf{x} - \mathbf{x}^0$ gives

$$\mathbf{x} - \mathbf{x}^0 \approx \left(J_{\mathbf{x}}^T(\mathbf{x}^0, \mathbf{q}^0) J_{\mathbf{x}}(\mathbf{x}^0, \mathbf{q}^0) \right)^{-1} J_{\mathbf{x}}^T(\mathbf{x}^0, \mathbf{q}^0) \left(\mathbf{r} - \mathbf{f}(\mathbf{x}^0, \mathbf{q}^0) - J_{\mathbf{q}}(\mathbf{x}^0, \mathbf{q}^0)(\mathbf{q} - \mathbf{q}^0) \right). \quad (23)$$

²See also physics.nist.gov/cuu/Uncertainty/, the web page of Physics laboratory of National Institute of Standards and Technology.

In reality, the measurements \mathbf{r} are disturbed by measurement errors \mathbf{e} such that $\mathbf{r} = \mathbf{r}^0 + \mathbf{e}$. Substituting this into (23) yields

$$\mathbf{x} - \mathbf{x}^0 \approx \left(J_{\mathbf{x}}^T(\mathbf{x}^0, \mathbf{q}^0) J_{\mathbf{x}}(\mathbf{x}^0, \mathbf{q}^0) \right)^{-1} J_{\mathbf{x}}^T(\mathbf{x}^0, \mathbf{q}^0) \left(\mathbf{e} - J_{\mathbf{q}}(\mathbf{x}^0, \mathbf{q}^0) (\mathbf{q} - \mathbf{q}^0) \right). \quad (24)$$

This is the result that allows to analyze the bias and covariance of the positioning error. The measurement errors \mathbf{e} are typically modeled as zero mean random variables with the covariance \mathbf{C}_e . Alternatively, the measurement errors may contain bias \mathbf{b}_e , which could be included into the systematic errors in the analysis what follows. The term

$$\mathbf{b}_r = J_{\mathbf{q}}(\mathbf{x}^0, \mathbf{q}^0) (\mathbf{q} - \mathbf{q}^0) \quad (+\mathbf{b}_e) \quad (25)$$

presents the measurement bias. The location bias resulting from the measurement bias (25) is

$$\mathbf{b} = - \left(J_{\mathbf{x}}^T(\mathbf{x}^0, \mathbf{q}^0) J_{\mathbf{x}}(\mathbf{x}^0, \mathbf{q}^0) \right)^{-1} J_{\mathbf{x}}^T(\mathbf{x}^0, \mathbf{q}^0) \mathbf{b}_r. \quad (26)$$

The positioning error covariance becomes

$$\mathbf{C} = \left(J_{\mathbf{x}}^T(\mathbf{x}^0, \mathbf{q}^0) J_{\mathbf{x}}(\mathbf{x}^0, \mathbf{q}^0) \right)^{-1} J_{\mathbf{x}}^T(\mathbf{x}^0, \mathbf{q}^0) \mathbf{C}_e J_{\mathbf{x}}(\mathbf{x}^0, \mathbf{q}^0) \left(J_{\mathbf{x}}^T(\mathbf{x}^0, \mathbf{q}^0) J_{\mathbf{x}}(\mathbf{x}^0, \mathbf{q}^0) \right)^{-1}. \quad (27)$$

It can be shown that \mathbf{C} may be upper bounded by

$$\mathbf{C}_u = n \sigma_e^2 \left(J_{\mathbf{x}}^T(\mathbf{x}^0, \mathbf{q}^0) J_{\mathbf{x}}(\mathbf{x}^0, \mathbf{q}^0) \right)^{-1}, \quad (28)$$

where n is the number of measurements (the dimension of \mathbf{r}) and σ_e^2 is the maximum (diagonal) element of \mathbf{C}_e . The upper bound is in the sense that the matrix difference $\mathbf{C}_u - \mathbf{C}$ is positive semidefinite. A tighter upper bound and a lower bound can be obtained by substituting $n \sigma_e^2$ by the maximum and minimum eigenvalues of \mathbf{C}_e , respectively.

It can be concluded that the mean squared error is upper bounded by

$$\mathbf{V}_u = n (b^2 + \sigma_e^2) \left(J_{\mathbf{x}}^T(\mathbf{x}^0, \mathbf{q}^0) J_{\mathbf{x}}(\mathbf{x}^0, \mathbf{q}^0) \right)^{-1}, \quad (29)$$

where b is the maximum diagonal element of $\mathbf{b}_r \mathbf{b}_r^T$. Equation (29) can be used to find an approximative performance of a location system after the maximum single measurement error bias b and maximum estimation error variance σ_e^2 have been evaluated. The term $\mathbf{Q} = \left(J_{\mathbf{x}}^T(\mathbf{x}^0, \mathbf{q}^0) J_{\mathbf{x}}(\mathbf{x}^0, \mathbf{q}^0) \right)^{-1}$ presents effects of the sensor geometry to the location accuracy and may be called as the geometric dilution of precision (GDOP) [34]. Reference [34] gives results related to it for the hyperbolic and direction finding location systems.

5.2 Hyperbolic Location

The hyperbolic location systems use differences of times-of-arrival (TOAs) measured either directly [65] or subtracting measured TOAs [34]. Therefore, they may be called time difference (TD) location systems. The methods require that the measuring node network is synchronized or nodes have known relations between their clocks. Let the transmission time be denoted as t_0 . The signal pass the distance $d_i^0 = \|\mathbf{x}^0 - \mathbf{x}_i^0\|$, where $\|\cdot\|$ denotes the Euclidean vector norm, between the emitter and the node i at \mathbf{x}_i at time τ_i . The receiver therefore observes the signal at time $t_i = t_0 + \tau_i + \delta_i$, where δ_i denotes the network synchronization error, i.e., the time difference to the common time of the positioning network. Let node j be a reference node. Subtracting t_j from the other measurements and multiplying the results with the propagation speed of the signal c the measurements of the hyperbolic location systems are modeled as

$$r_i = c(t_i - t_j) = \|\mathbf{x} - \mathbf{x}_i\| - \|\mathbf{x} - \mathbf{x}_j\| + c(\delta_i - \delta_j) + e_i. \quad (30)$$

If there are N nodes, then there are $N - 1$ measurements the minimum possible number being $N = D + 1$, where D is the dimension of the location problem, i.e., two or three.

Often, in UWB, the round trip time (RTT) is used since precise network synchronization is a challenging task in sensor networks. In the RTT a message is sent to a target which retransmits it (or corresponding response) back. The time difference between transmission and reception is $\Delta = 2\tau + T_{\text{process}}$, where the latter is the processing time spend by the target. If this is not precisely known a similar effect to network synchronization error occurs. Therefore, the following analysis based on network synchronization error is valid also for RTT measurements.

Clearly, the system parameters $\mathbf{q} = [\mathbf{x}_1^T \dots \mathbf{x}_N^T \delta_1 \dots \delta_N]^T$ include the locations of the nodes \mathbf{x}_i and the clock errors δ_i . The actual node locations are \mathbf{x}_i^0 . The presumed node locations may differ from the actual positions by $\delta_{\mathbf{x}_i}$. The desired value δ_i^0 for the clock errors is naturally zero. For brevity, let $J_{\mathbf{x}} = J_{\mathbf{x}}(\mathbf{x}^0, \mathbf{q}^0)$. Then, the Jacobian with respect to the unknown location is

$$J_{\mathbf{x}} = \begin{bmatrix} \frac{(\mathbf{x}^0 - \mathbf{x}_1^0)^T}{d_1^0} - \frac{(\mathbf{x}^0 - \mathbf{x}_j^0)^T}{d_j^0} \\ \vdots \\ \frac{(\mathbf{x}^0 - \mathbf{x}_{j-1}^0)^T}{d_{j-1}^0} - \frac{(\mathbf{x}^0 - \mathbf{x}_j^0)^T}{d_j^0} \\ \frac{(\mathbf{x}^0 - \mathbf{x}_{j+1}^0)^T}{d_{j+1}^0} - \frac{(\mathbf{x}^0 - \mathbf{x}_j^0)^T}{d_j^0} \\ \vdots \\ \frac{(\mathbf{x}^0 - \mathbf{x}_N^0)^T}{d_N^0} - \frac{(\mathbf{x}^0 - \mathbf{x}_j^0)^T}{d_j^0} \end{bmatrix}. \quad (31)$$

The i th element of the bias $\mathbf{b}_{\mathbf{r}}$ is

$$[\mathbf{b}_{\mathbf{r}}]_i = \frac{-(\mathbf{x}^0 - \mathbf{x}_i^0)^T \delta_{\mathbf{x}_i}}{d_i^0} + \frac{(\mathbf{x}^0 - \mathbf{x}_j^0)^T \delta_{\mathbf{x}_j}}{d_j^0} + c(\delta_i - \delta_j). \quad (32)$$

The terms may be contrastive resulting in a small bias. The terms may, as well, be restorative resulting in a large bias. The clock error term, the last term in (32), attains its maximum if the clock errors are to opposite directions and minimum if the clock errors are to the equal direction. If the clock error $\delta_i - \delta_j$ is 3 ns, 1 μ s or 1 ms and the signal is a radio signal, then the caused biases are 1 m, 300 m and 300 km, respectively. The clock errors may therefore be rather fatal to the accuracy of the hyperbolic location systems and clearly show why very accurate network synchronization is required in these systems.

Due to the Schwartz inequality the first two terms in (32) are bounded as

$$\|(\mathbf{x}^0 - \mathbf{x}_i^0)^T \delta_{\mathbf{x}_i}\|/d_i^0 \leq \frac{1}{d_i^0} \|(\mathbf{x}^0 - \mathbf{x}_i^0)\| \|\delta_{\mathbf{x}_i}\| = \|\delta_{\mathbf{x}_i}\|,$$

with equality if and only if $\delta_{\mathbf{x}_i} = \alpha(\mathbf{x}^0 - \mathbf{x}_i^0)$, where α is a constant. Consequently, the errors through the node locations are at maximum if $\delta_{\mathbf{x}_i}$ are parallel to $\mathbf{x}^0 - \mathbf{x}_i^0$. These errors vanish if $\delta_{\mathbf{x}_i}$ and $\mathbf{x}^0 - \mathbf{x}_i^0$ are orthogonal. The bias due to node location errors are not necessarily very large since the sensors (or base stations) can typically be set within few meters. However, the sensor location accuracy can not be larger than the accuracy required from the system. Otherwise, the bias through the sensor location accuracy may dominate the error budget.

The accuracy may be approximated, as already explained, by calculating the GDOP term for different positioning geometry using the Jacobian \mathbf{J}_x , the bias b and measurement error variance. The first two terms were just discussed, the next one will be discussed in the next section.

5.3 Delay Estimation Accuracy

The accuracy of the delay estimator can be estimated by the Cramér-Rao bound (CRB). Assuming a half sinusoidal chip waveform, the standard deviation of the delay estimator according to the CRB becomes

$$\sigma_\tau = \frac{1}{\sqrt{2N\pi^2\gamma}} T_p, \quad (33)$$

where T_p is the pulse duration, N is the number of used pulses and γ is the SNR of a pulse. Since the pulse duration is rather short in UWB (less than 3 ns), i.e., 1 m in distance, the obtainable accuracy will be good assuming that geometry (GDOP) is favorable for positioning and bias is small.

Typical delay estimator includes a correlator and a delay lock loop. In packet based system such may be inadequate and, preferably, the maximum output of the correlator is searched. Therein, the interpolation techniques may increase the accuracy. In a interpolation technique a parabola is fitted to the maximum and its neighboring samples [66–68]. Let k denote the sample index of the maximum, $c(k)$, $c(k-1)$, $c(k+1)$ the maximum value of the envelope of the correlator's output and its neighbors. Then, the corrected delay estimate is

$$\hat{\tau} = \left(k + \frac{1}{2} \frac{c(k-1) - c(k+1)}{c(k-1) - 2c(k) + c(k+1)} \right) \frac{T_c}{q}. \quad (34)$$

More details about interpolation effects may be found from [69].

6 Conclusions

This chapter comprehensively studied localization in cellular/sensor networks by making use of UWB technology. It covered several topics including TOA estimation, positioning approaches, and positioning accuracy. Also included are the authors' recent contributions.

To exploit the fine time resolution of UWB signals, TOA/TDOA measurements should be employed to locate UWB devices. For low cost and low complexity applications, the presented non-coherent TOA estimation scheme may be employed. On the other hand, the proposed two stage approach could be considered to achieve rapid acquisition and high accuracy, especially for low data rate scenarios. A trade-off between complexity and accuracy needs to be dealt with in choosing a positioning algorithm for practice of interest. In evaluating positioning performance, systematic errors should be taken into account to provide a more realistic performance reference.

Acknowledgement

This work is partly funded by the EU 6th framework project PULSERS.

References

- [1] R. J. Fontana, "Recent system applications of short-pulse ultra-wideband (UWB) technology," *IEEE Trans. Microwave Theory and Tech.*, vol. 52, no. 9, pp. 2087–2104, 2004.
- [2] R. J. Fontana, E. Richley, and J. Barney, "Commercialization of an ultra wideband precision asset location system," in *Proc. IEEE Conf. UWB systems and Technologies*, 2003.
- [3] I. Oppermann, L. Stoica, A. Rabbachin, Z. Shelby, and J. Haapola, "UWB wireless sensor networks: UWEN—a practical example," *IEEE Communications Magazine*, vol. 42, pp. 527–532, Dec. 2004.
- [4] K. Yu, J. P. Montillet, A. Rabbachin, P. Cheong, and I. Oppermann, "UWB location and tracking for wireless embedded networks," *EURASIP Journal of Signal Processing, Special Issue on Signal Processing in UWB Communications*, to appear.
- [5] M. Mauve, J. Widmer, and H. Hartenstein, "A survey on position based routing in mobile ad-hoc networks," *IEEE network Magazine*, vol. 15, pp. 30–39, Nov.-Dec. 2001.

- [6] X. Li, *Super Resolution TOA Estimation with Diversity Techniques for Indoor Geolocation Applications*. PhD thesis, Worcester Polytechnic Institute, 2003.
- [7] E. A. Homier and R. A. Scholtz, "Rapid acquisition of ultra-wideband signals in the dense multipath channel," in *Proc. IEEE 2nd Ultra Wideband Systems and Technologies (UWBST'02)*, pp. 245–249, May 2002.
- [8] R. Fleming, C. Kushner, G. Roberts, and U. Nandiwada, "Rapid acquisition for ultra-wideband localizers," in *Proc. IEEE 2nd Ultra Wideband Systems and Technologies (UWBST'02)*, pp. 105–109, May 2002.
- [9] I. Maravic, M. Vetterli, and K. Ramchandran, "Channel estimation and synchronization with subnyquist sampling and application to ultra-wideband systems," in *Proc. IEEE Symposium on Circuits and Systems (ISCAS)*, (Vancouver, Canada), pp. 381–384, May 2004.
- [10] J.-Y. Lee and R. A. Scholtz, "Ranging in a dense multipath environment using an uwb radio link," *IEEE J. Select. Areas Commun.*, vol. 20, pp. 1677 – 1683, Dec. 2002.
- [11] M. Weisenhorn and W. Hirt, "Robust noncoherent receiver exploiting UWB channel properties," in *Proc. Joint UWBST&IWUWBS*, vol. 2, pp. 156–160, May 2004.
- [12] Y. Nakache, P. Orlik, W. Gifford, A. Molisch, I. Ramachandran, G. Fang, and J. Zhang, "Low-complexity ultrawideband transceiver with compatibility to multiband-OFDM," in *Proc. Joint UWBST&IWUWBS*, pp. 151–155, May 2004.
- [13] A. Rabbachin, R. Tesi, and I. Oppermann, "Bit error rate analysis for UWB systems with a low complexity, non-coherent energy collection receiver," in *Proc. IST Mobile & Wireless Communications Summit*, vol. 1, pp. 223–227, June 2004.
- [14] T. Q. S. Quek and M. Z. Win, "Ultrawide bandwidth transmitted-reference signaling," in *Proc. IEEE International Conference on Communications (ICC)*, vol. 6, pp. 3409–3413, June 2004.
- [15] R. Hooctor and H. Tomlinson, "Delay hopped transmitted reference experimental results," in *Proc. IEEE 2nd Ultra Wideband Systems and Technologies (UWBST'02)*, pp. 93–98, May 2002.
- [16] R. Hooctor and H. Tomlinson, "Delay-hopped transmitted-reference RF communications," in *Proc. IEEE 2nd Ultra Wideband Systems and Technologies (UWBST'02)*, pp. 265–269, May 2002.
- [17] J. D. Choi and W. E. Stark, "Performance of ultra-wideband communications with suboptimal receivers in multipath channels," vol. 20, pp. 1754–1766, Dec. 2002.

- [18] K. Yu and I. Oppermann, "Timing acquisition and position estimation for IR-UWB wireless sensor networks," *submitted to IEEE JSAC special issue on ultra wideband wireless communications—theory and applications*, Mar. 2005.
- [19] S. M. Kay, *Fundamentals of Statistical Signal Processing: Detection Theory*. Upper Saddle River, NJ: Prentice Hall, 1998.
- [20] J. G. Proakis, *Digital Communications*. McGraw-Hill, 3rd ed., 1995.
- [21] A. Polydoros and C. L. Weber, "A unified approach to serial search spread-spectrum code acquisition-part II: a matched-filter receiver," *IEEE Trans. Commun.*, vol. 32, pp. 550–560, May 1984.
- [22] E. Sourour and S. C. Gupta, "Direct-sequence spread-spectrum parallel acquisition in nonselective and frequency-selective Rician fading channels," *IEEE J. Select. Areas Commun.*, vol. 10, pp. 535–544, Apr. 1992.
- [23] B. T. Fang, "Simple solutions for hyperbolic and related position fixes," *IEEE Trans. Aerosp. Electron. Syst.*, vol. 26, pp. 748–753, Sept. 1990.
- [24] K. Yu and I. Oppermann, "Performance of UWB position estimation based on TOA measurements," in *Proc. Joint UWBST & IWUWBS*, (Kyoto, Japan), pp. 400–404, 2004.
- [25] J. O. Smith and J. S. Abel, "Closed-form least squares source location estimation from range difference measurements," *IEEE Trans. Acoust. Speech, Signal Processing*, vol. 35, pp. 1661–1669, Dec. 1987.
- [26] B. Friedlander, "A passive localization algorithm and its accuracy analysis," *IEEE J. Ocean. Eng.*, vol. 12, pp. 234–245, Jan. 1987.
- [27] H. C. Schau and A. Z. Robinson, "Passive source location employing intersecting spherical surfaces from time-of-arrival differences," *IEEE Trans. Acoust. Speech, Signal Processing*, vol. 35, pp. 1223–1225, Aug. 1987.
- [28] Y. T. Chan and K. C. Ho, "A simple and efficient estimator for hyperbolic location," *IEEE Trans. Signal Processing*, vol. 42, pp. 1905–1915, Aug. 1994.
- [29] Y. Huang, J. Benesty, G. W. Elko, and R. M. Mersereau, "Real-time passive source localization: a practical linear-correction least-squares approach," *IEEE Trans. Speech and Audio Processing*, vol. 9, pp. 943–956, Nov. 2001.

- [30] D. Niculescu and B. Nath, “Ad hoc positioning system (APS),” in *Proc. IEEE GLOBECOM*, (San Antonio, TX, USA), pp. 2926–2931, 2001.
- [31] A. Savvides, C.-C. Han, and M. B. Strivastava, “Dynamic fine-grained localization in ad-hoc networks of sensors,” in *Proc. ACM SIGMOBILE*, (Rome, Italy), pp. 166–179, 2001.
- [32] K. Langendoen and N. Reijers, “Distributed localization in wireless sensor networks: a quantitative comparison,” *Computer Networks*, vol. 43, pp. 499–518, 2003.
- [33] W. H. Foy, “Position-location solutions by Taylor-series estimation,” *IEEE Trans. Aerosp. Electron. Syst.*, vol. 12, pp. 187–194, Mar. 1976.
- [34] D. J. Torieri, “Statistical theory of passive location systems,” *IEEE Trans. Aerosp. Electron. Syst.*, vol. 20, pp. 183–198, Mar. 1984.
- [35] D. E. Manolakis, “Efficient solution and performance analysis of 3-D position estimation by trilateration,” *IEEE Trans. Aerosp. Electron. Syst.*, vol. 32, pp. 1239–1248, Oct. 1996.
- [36] M. A. Spirito, “On the accuracy of cellular mobile station location estimation,” *IEEE Trans. Veh. Technol.*, vol. 50, pp. 674–685, May 2001.
- [37] K. W. Cheung, H. C. So, W. K. Ma, and Y. T. Chan, “Least squares algorithms for time-of-arrival-based mobile location,” *IEEE Trans. Signal Processing*, vol. 52, pp. 1121–1128, Apr. 2004.
- [38] P. E. Gill, W. Murray, and M. H. Wright, *Practical Optimization*. London: Academic Press, 1981.
- [39] R. Fletcher, *Practical Methods of Optimization*. Chichester: John Wiley & Sons, 1987.
- [40] S. Boyd and L. Vandenberghe, *Convex Optimization*. Cambridge University Press, 2004.
- [41] J. J. Caffery and G. L. Stuber, “Overview of radiolocation in CDMA cellular systems,” *IEEE Commun. Magazine*, pp. 38–45, May 1998.
- [42] D. Marquardt, “Algorithm for least-squares estimation of nonlinear parameters,” *SIAM J. Appl. Math.*, vol. 11, pp. 431–441, 1963.
- [43] K. Yu and I. Oppermann, “UWB positioning for wireless embedded networks,” in *Proc. IEEE RAWCON*, (Atlanta, USA), 2004.
- [44] L. Doherty, K. S. J. Pister, and L. E. Ghaoui, “Convex position estimation in wireless sensor networks,” in *IEEE INFOCOM*, pp. 1655–1663, 2001.
- [45] J. Nelder and R. Mead, “A simplex method for function minimization,” *Computer Journal*, vol. 7, pp. 308–313, 1965.

- [46] H. Wu, C. Wang, and N.-F. Tzeng, "Novel self-configurable positioning technique for multi-hop wireless network," *IEEE Trans. Networking*, submitted for publication.
- [47] M. Hellebrandt and R. Mathar, "Location tracking of mobiles in cellular radio networks," *IEEE Trans. Veh. Technol.*, vol. 48, pp. 1558–1562, Sept. 1999.
- [48] M. McGuire and K. Plataniotis, "Dynamic model-based filtering for mobile terminal location estimation," *IEEE Trans. Veh. Technol.*, vol. 52, pp. 1012–1031, July 2003.
- [49] M. Hellebrandt, R. Mathar, and M. Scheibenbogen, "Estimating position and velocity in a cellular radio network," *IEEE Trans. Veh. Technol.*, vol. 46, pp. 65–71, Feb. 1997.
- [50] P. Biswas and Y. Ye, "Semidefinite programming for ad hoc wireless sensor network localization," in *Proc. IEEE Information Processing in Sensor Networks (IPSN)*, pp. 46 – 54, Apr. 2004.
- [51] X. Li, H. Shi, and Y. Shang, "A map-growing localization algorithm for ad-hoc wireless sensor networks," in *Proc. IEEE Parallel and Distributed Systems,(ICPADS)*, pp. 395–402, July 2004.
- [52] X. g. Ji and H. Zha, "Sensor positioning in wireless ad-hoc sensor networks using multidimensional scaling," in *Proc. IEEE INFOCOM 2004, Twenty-third Annual Joint Conference of the IEEE Computer and Communications Societies*, vol. 4, pp. 2652–2661, Mar. 2004.
- [53] Y. Shang, J. Meng, and H. Shi, "A new algorithm for relative localization in wireless sensor networks," in *Proc. IEEE Parallel and Distributed Processing Symposium*, pp. 26–30, Apr. 2004.
- [54] T. He, C. Huang, B. M. Blum, J. Stankovic, and T. Abdelzaher, "Range-free localization schemes for large scale sensor networks," in *Proc. IEEE Mobicom 2003*, pp. 81–95, Sept. 2003.
- [55] D. Niculescu and B. Nath, "Ad hoc positioning system (aps) using aoa," in *Proc. IEEE Twenty-Second Annual Joint Conference of the IEEE Computer and Communications Societies (INFOCOM)*, vol. 3, pp. 1734 – 1743, Apr. 2003.
- [56] R. Nagpal, H. Shrobe, and J. Bachrach, "Organizing a global coordinate system from local information on an ad-hoc sensor network," in *Proc. International Workshop on Information Processing in Sensor Networks*, Apr. 2003.
- [57] S. Capkun, M. Hamidi, and J. P. Hubaux, "Gps-free positioning in mobile ad-hoc networks," in *Proc. IEEE Proceedings of the Hawaii International Conference on System Sciences, (Maui,HW)*, pp. 3481 – 3490, Jan. 2001.

- [58] D. Moore, J. Leonard, D. Rus, and S. Teller, “Robust distributed network localization with noisy range measurements,” in *Proc. ACM SenSys’04*, (Baltimore, Maryland, USA), pp. 50 – 61, Nov. 2004.
- [59] R. Iyengar and B. Sikdar, “Scalable and distributed gps free positioning for sensor networks,” in *Proc. IEEE ICC’03*, vol. 1, pp. 338 – 342, May11-15 2003.
- [60] Y. Zhang and L. Cheng, “Place: Protocol for location and coordinate estimationa wireless sensor network approach,” *Computer Networks*, vol. 46, pp. 679 – 693, July 2004.
- [61] C. Poggi and G. Mazzini, “Collinearity for sensor network localization,” in *Proc. IEEE Vehicular Technology Conference, VTC 2003-Fall*, vol. 5, pp. 3040–3044, Oct. 2003.
- [62] J.-C. Chen, C.-S. Maa, Y.-C. Wang, and J.-T. Chen, “Mobile position location using factor graphs,” *IEEE Electronic Letters*, vol. 7, no. 9, pp. 431 – 433, 2003.
- [63] D. Kaplan, *Understanding GPS Principles and Applications*. Boston: Artech House, 1996.
- [64] J. R. Taylor, *An Introduction to Error Analysis: the Study of Uncertainties in Physical Measurements*. University Science Books, second edition, 1997.
- [65] G. C. Carter, “Time delay estimation for passive sonar signal proessing,” *IEEE Transactions on Acoustics, Speech, and Signal Processing*, vol. 29, pp. 463–470, June 1981.
- [66] R. Moddemeijer, “On the determination of the position of extrema of sampled correlators,” *IEEE Trans. Signal Processing*, vol. 39, pp. 216–219, Jan. 1991.
- [67] G. Jacovitti and G. Scarano, “Discrete time techniques for time delay estimation,” *IEEE Trans. Signal Processing*, vol. 41, pp. 525–533, Feb. 1993.
- [68] G. Giunta, “Fast estimation of time delay and doppler stretch based on discrete-time methods,” *IEEE Trans. Signal Processing*, vol. 46, pp. 1785–1797, July 1998.
- [69] H. Saarnisaari, “Some design aspects of mobile local positioning systems,” in *Proc. of the IEEE Position Location and Navigation Symposium*, (Monterey, CA, USA), pp. 1688–1692, 20024.